

# Adaptive Control for Rejecting Disturbances with Time-varying Frequencies in Tape Systems

Hua Zhong, Vishwesh Kulkarni, and Lucy Pao

**Abstract**—In this paper, we present two adaptive algorithms for tape systems that account for tape tension ripples. Tape tension ripples are caused by reel eccentricities that produce disturbances with time-varying frequencies. In both designs, the frequency and the magnitude of the disturbance are estimated to synthesize an input signal to cancel the disturbance. In the first design, by adjusting the values of the adaptive parameters that are related to the frequency of the disturbance, the estimated frequency reflects the time-varying nature of the disturbance. The second design extends an existing digital adaptive feed-forward cancellation scheme used in hard disk drives for application to tape tension control problems. For both designs, time-varying sinusoidal disturbance signals are used in simulations to analyze and evaluate the performances of the developed adaptive control methods on a model of a tape system.

## I. INTRODUCTION

In tape systems, reel eccentricities cause ripples in tape tension and can permanently damage the tape. The disturbances are quasi-periodic with frequencies varying slowly, typically within the range from 20 Hz to 60 Hz, as the radii of the two reels change as tape winds from one reel to the other. Naturally, the frequencies of the disturbances are a function of the tape tangential velocities and the reel radii. How to cancel the disturbances from reel eccentricities with time-varying frequencies is a challenging task in the control of tape systems.

There has been some research conducted on rejecting sinusoidal disturbances. Most of the work is based on the internal model principle (IMP) [6], which states that a system can perfectly reject disturbances at some frequency and track the reference with zero steady-state error if a model of the disturbance generator is included internally in the closed-loop system. If we know the frequency of the disturbance, the disturbance can be effectively cancelled by estimating the magnitude and the phase of the signal and adding the inverse signal of the disturbance to the system [4][12]. Otherwise, we have to estimate the magnitude, phase, and frequency to synthesize the compensating signal. Based on the IMP, repetitive control and adaptive feed-forward cancellation are the two commonly applied approaches in rejecting periodic disturbances. Both of these methods can be extended easily to reject periodic disturbances that have a finite number of harmonic components. Repetitive control [8] has been designed to reject periodic disturbances with

fixed frequencies. Adaptive feed-forward cancellation has also been proven to be an effective technique to cancel periodic disturbances with multiple harmonics of either known or unknown but fixed frequencies [2][5]. An adaptive algorithm to compensate roll non-circularity perturbations with measured frequencies in web transport systems was developed in [13].

There are several issues of practical importance that the above algorithms should be extended to address. First, little has been published about rejection of disturbances with time-varying frequencies such as reel eccentricity disturbances in tape systems. Second, these algorithms have primarily only been developed for linear time-invariant (LTI) systems. However, tape systems are time-varying because the motion of the tape impacts the parameters and the characteristics of the system dynamics.

In this paper, we present two adaptive control algorithms that take into account the time-varying reel eccentricity disturbances in tape systems. The first approach extends the LTI feedback compensator technique in [2] for the time-varying tape system in which the disturbance is considered as an input disturbance. The second approach modifies an adaptive disturbance cancellation algorithm used in disk drives [7] to reject output disturbances with time-varying frequencies in tape systems.

This paper is organized as follows: Section II first introduces a state-space model for tape systems and then reviews a decoupled tape tension loop that we use in this research. Characteristics of and problems caused by reel eccentricity disturbances in tape systems are also discussed. Section III outlines the two extended control algorithms for rejecting disturbances with time-varying frequencies in tape systems. To simplify the analysis, we discuss the control schemes to cancel one disturbance from one reel and similar analysis can be applied to the disturbance from the other reel. Simulation results of these two control schemes are also presented. Finally, Section IV provides conclusions and discusses areas for future work.

## II. REEL ECCENTRICITIES IN TAPE SYSTEMS

### A. Tape System Model

The schematic in Fig. 1 illustrates a lumped-parameter model of a tape system. The unsupported length of tape is modeled by a parallel dashpot and spring with parameters  $D$  and  $K$ , respectively.  $J_i(t)$ ,  $r_i(t)$ , and  $\omega_i(t)$  are the inertia, radius, and angular velocity of each reel, respectively, for  $i = 1, 2$ . Define  $T(t)$  as the tape tension and  $V_i(t)$  as the tangential velocity of the tape at each reel. Let  $X=[T(t),$

This work was supported in part by the Colorado Center for Information Storage.

The authors are with the Electrical and Computer Engineering Department, University of Colorado at Boulder, Boulder, CO. Email: zhongh@colorado.edu; vishwesh@colorado.edu; pao@colorado.edu.

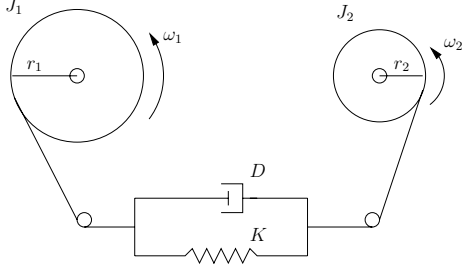


Fig. 1. Lumped-parameter model of a tape system.

$V_1(t)$ ,  $V_2(t)$ ]<sup>T</sup> and  $U=[u_1(t), u_2(t)]$ <sup>T</sup>. Here,  $u_i(t)$  is the current applied to each DC motor to drive each reel. A non-linear time-varying model of tape systems is derived in [1] with special consideration for air entrainment effects in tape systems. However, because we are interested in reel eccentricity disturbance control, we address steady-state rather than transient control of the tape system. In steady-state, air entrainment becomes constant and thus  $K$  and  $D$  are constant. Hence, the time-varying dynamics accounted for here are only from the radii and the inertia:

$$\dot{X}(t) = \mathbf{A}(t)X(t) + \mathbf{B}(t)u(t) + \frac{\epsilon}{2\pi} \mathbf{d}(t), \quad (1)$$

with

$$\mathbf{A}(t) = \begin{bmatrix} -D \left( \frac{r_1^2(t)}{J_1(t)} + \frac{r_2^2(t)}{J_2(t)} \right) & D \left( \frac{\beta_1}{J_1(t)} - \sigma \right) & D \left( \sigma - \frac{\beta_2}{J_2(t)} \right) \\ \frac{r_1^2(t)}{J_1(t)} & -\frac{\beta_1}{J_1(t)} & 0 \\ -\frac{r_2^2(t)}{J_2(t)} & 0 & -\frac{\beta_2}{J_2(t)} \end{bmatrix},$$

$$\mathbf{B}(t) = \begin{bmatrix} -D \frac{r_1(t)K_{t1}}{J_1(t)} & D \frac{r_2(t)K_{t2}}{J_2(t)} \\ \frac{r_1(t)K_{t1}}{J_1(t)} & 0 \\ 0 & \frac{r_2(t)K_{t2}}{J_2(t)} \end{bmatrix},$$

$$\mathbf{d} = \begin{bmatrix} D \left( \frac{V_1^2(t)}{r_1^2(t)} \left( 1 - \frac{4K_J r_1^4(t)}{J_1(t)} \right) + \frac{V_2^2(t)}{r_2^2(t)} \left( 1 - \frac{4K_J r_2^4(t)}{J_2(t)} \right) \right) \\ -\frac{V_1^2(t)}{r_1^2(t)} \left( 1 - \frac{4K_J r_1^4(t)}{J_1(t)} \right) \\ \frac{V_2^2(t)}{r_2^2(t)} \left( 1 - \frac{4K_J r_2^4(t)}{J_2(t)} \right) \end{bmatrix},$$

where  $\mathbf{d}$  is a function of  $X$ ,  $\epsilon$  is the thickness of the tape,  $\sigma$  equals to  $\frac{K}{D}$ ,  $K_J$  is the inertia constant of the tape pack and is determined by  $\epsilon$  and the tape density  $t_\rho$ ,  $K_{ti}$  is the torque constant of each motor, and  $\beta_i$  is the motor viscosity coefficient. Notice that the matrix  $\mathbf{B}(t)$  can be written as the product of one constant matrix  $\mathbf{B}_0$  and one time-varying matrix  $\mathbf{B}_1(t)$ :

$$\mathbf{B}(t) = \begin{bmatrix} -D & D \\ 1 & 0 \\ 0 & 1 \end{bmatrix} \begin{bmatrix} \frac{r_1(t)K_{t1}}{J_1(t)} & 0 \\ 0 & \frac{r_2(t)K_{t2}}{J_2(t)} \end{bmatrix} \doteq \mathbf{B}_0 \mathbf{B}_1(t).$$

As in [1], we first transform the state equation (1) to an error system state equation by changing the state variables.

Let  $e_x(t)=[e_T(t), e_{V_1}(t), e_{V_2}(t)]$ <sup>T</sup>  $=[T(t) - T_d, V_1(t) - V_d, V_2(t) - V_d]$ <sup>T</sup> with  $V_d$  and  $T_d$  denoting the desired tangential velocity and tension of the tape, respectively. The error system state equation can be written as

$$\dot{e}_x = \mathbf{A}(t)e_x + \mathbf{B}(t)u_a(t)$$

where

$$u_a(t) = u(t) - \mathbf{B}_1^{-1}(t)u_0(t)$$

and

$$u_0(t) = \mathbf{B}_1(t) \begin{bmatrix} -\frac{r_1(t)}{K_{t1}} T_d + \frac{\beta_1}{r_1(t)K_{t1}} V_d \\ + \frac{\epsilon}{2\pi} \frac{V_1^2(t)J_1}{r_1^3(t)K_{t1}} \left( 1 - 4 \frac{K_J r_1^4(t)}{J_1(t)} \right) \\ \frac{r_2(t)}{K_{t2}} T_d + \frac{\beta_2}{r_2(t)K_{t2}} V_d \\ - \frac{\epsilon}{2\pi} \frac{V_2^2(t)J_2}{r_2^3(t)K_{t2}} \left( 1 - 4 \frac{K_J r_2^4(t)}{J_2(t)} \right) \end{bmatrix},$$

to cancel the components with  $T_d$ ,  $V_d$ , and  $\mathbf{d}$ .

Then we linearize this equation by state feedback with a time-varying feedback gain matrix  $\mathbf{M}(t)$ . The feedback law is

$$u_a(t) = \mathbf{B}_1^{-1}(t)(\mathbf{M}(t)e_x + u_e(t))$$

where

$$\mathbf{M}(t) = \begin{bmatrix} -p - \frac{r_1^2(t)}{J_1(t)} & q + \frac{\beta_1}{J_1(t)} & c \\ p + \frac{r_2^2(t)}{J_2(t)} & c & q + \frac{\beta_2}{J_2(t)} \end{bmatrix}$$

and

$$u_e(t) = \mathbf{B}_1(t)u(t) - u_0(t) - \mathbf{M}(t)e_x(t).$$

Here,  $p$ ,  $q$ , and  $c$  are constant feedback gains. Now the error system state equation becomes

$$\dot{e}_x = \mathbf{A}_0 e_x + \mathbf{B}_0 u_e(t),$$

where

$$\mathbf{A}_0 = \begin{bmatrix} 2Dp & D(c - q - \sigma) & -D(c - q - \sigma) \\ -p & q & c \\ p & c & q \end{bmatrix}.$$

## B. Decoupled Tension Loop

Decoupled tension and velocity loops taking into account air entrainment and motor parameter uncertainties are described in [1]. Here, we use a simplified decoupled tension loop that excludes air entrainment and assumes motor parameters are well characterized. Define  $e(t)=[e_T(t), e_W(t), e_V(t)]$ <sup>T</sup> and  $u_d(t)=[u_{d1}(t), u_{d2}(t)]$  where

$$e_W(t) = \frac{e_{V_1}(t) - e_{V_2}(t)}{2},$$

$$e_V(t) = \frac{e_{V_1}(t) + e_{V_2}(t)}{2},$$

$$u_{d1}(t) = \frac{u_{e2}(t) - u_{e1}(t)}{2},$$

$$u_{d2}(t) = \frac{u_{e1}(t) + u_{e2}(t)}{2}.$$

Then the tension loop consisting of the  $e_T$  and  $e_W$  states is perfectly decoupled from  $e_V(t)$ :

$$\begin{bmatrix} \dot{e}_T \\ \dot{e}_W \end{bmatrix} = \begin{bmatrix} 2Dp & 2D(c-q-\sigma) \\ -p & q-c \end{bmatrix} \begin{bmatrix} e_T \\ e_W \end{bmatrix} + \begin{bmatrix} 2D \\ -1 \end{bmatrix} u_{d1}(t). \quad (2)$$

It has been proven in [1] that the tension error  $e_T$  is guaranteed to go to zero if the feedback gains are under the restriction

$$\begin{aligned} p &< 0, \\ 0 &< c - q < \sigma, \end{aligned}$$

and  $u_{d1}$  is chosen such that

$$\text{sign}\{u_{d1}\} = -\text{sign}\left\{e_T - e_W \frac{c - q - \sigma}{p}\right\}. \quad (3)$$

### C. Reel Eccentricities

When tape winds from the source reel to the takeup reel, the eccentricities of both reels introduce tension ripples, and this can cause the tape to wind onto the takeup reel in an uneven fashion. Tension ripples can cause lateral shifts in the tape that can lead to permanent damage to the edges of the tape, which results in data loss. The magnitude of the ripple  $\Delta T$  in the tension depends on the spring constant  $K$  and the deviation amount of the pack radius  $\Delta r$  [10]:

$$\Delta T = 2\pi\Delta rK. \quad (4)$$

The frequencies of the reel eccentricity disturbances are integer multiples of the rotating frequency  $\omega_i(t)$  ( $i = 1, 2$ ) of the corresponding reel, which varies with the change in pack radius because the tangential velocity of the tape is controlled to be constant. Considering the takeup reel as an example, the radius of this reel increases and thus its angular velocity decreases during operation, so the frequency of the disturbance from the takeup reel decreases. The opposite happens in the source reel.

Consider a tape system with parameters as in Table I [11], where the motor torque constant  $K_t$  and the viscosity coefficients  $\beta$  are identical for both reels. Initially, the empty takeup reel has a radius  $r_2=0.014$  m and the radius of the full source reel is  $r_1=0.028$  m. With a desired tape velocity  $V_d$  of 5 m/sec and using an approximate estimation based on a linear time-invariant tape model shows that when the tape is wound from the full source reel to the empty takeup reel, the dominant frequency of the disturbance from the takeup reel varies from  $\omega_1=357$  rad/sec to  $\omega_2=178$  rad/sec, so  $\Delta\omega=179$  rad/sec. It is clear that the frequency of the disturbance is time-varying.

In this research, we assume the disturbances are pure sinusoid signals at the reel rotating frequency. Future work will generalize the control schemes to reject reel eccentricity disturbances consisting of multiple (potentially  $>10$ ) frequencies with validation on tape reel runout data from the tape industry.

TABLE I  
TAPE SYSTEM PARAMETERS FOR SIMULATION

Parameter	Label	Value
Tape density	$t_\rho$	1.6e3 kg/m <sup>3</sup>
Thickness of the tape	$\epsilon$	10e-5 m
Initial radius of reel 1	$r_1(0)$	0.028 m
Initial radius of reel 2	$r_2(0)$	0.014 m
Inertia of the reel	$J$	2.6e-5 kg m <sup>2</sup>
Tape pack inertia constant	$K_J$	20.14 kg/m <sup>2</sup>
Dashpot constant	$D$	0.9 N sec/m
Spring constant	$K$	630 N/m
Motor torque constant	$K_t$	0.016 N m/Amp
Motor viscosity coefficient	$\beta$	2.57e-5 N m sec/rad

## III. ADAPTIVE CONTROL ALGORITHMS AND SIMULATION RESULTS

This section presents two adaptive algorithms for rejecting time-varying disturbances based on methods originally presented in [2] and [7].

### A. Tape system model for simulations

For the simulations, we use the decoupled tension loop described in equations (2) and (3):  $P$  is the tape system plant along with its basic compensating controller and the output is the tension error. With parameters of the tape system set as in Table I, the constant feedback gains are selected following the guidelines in [1] to be  $p = -500$ ,  $q = -338$ , and  $c = 312$ . The decoupled tension loop is then

$$\begin{aligned} \begin{bmatrix} \dot{e}_T \\ \dot{e}_W \end{bmatrix} &= \begin{bmatrix} -900 & -90 \\ 500 & -650 \end{bmatrix} \begin{bmatrix} e_T \\ e_W \end{bmatrix} + \begin{bmatrix} 1.8 \\ -1 \end{bmatrix} u_{d1}(t), \\ u_{d1} &= -\text{sign}\{e_T - 0.1e_W\}, \end{aligned}$$

and

$$P(s) = \frac{1.8s + 1260}{s^2 + 1550s + 630000}.$$

Variations in the radius around each reel cause variations in the tape tangential velocity at each reel and hence cause disturbances in the tension. Thus, reel eccentricity can be thought of either (A) as an input disturbance to the tension loop equations (2) and (3), as will be considered in section III-B or (B) as an output disturbance on the tension based upon the relations given in equation (4), as will be considered in section III-C.

### B. Time-varying Controller Design

In this analysis, the disturbance from reel eccentricities is equivalent to an input disturbance:

$$d(t) = A_d \cos(\omega_d(t)t), \quad \dot{\omega}_d(t) = a.$$

The frequency of the disturbance varies linearly at a rate  $a$ . A time-varying controller is needed to reject the disturbance and keep the tension following the reference as shown in Fig. 2.

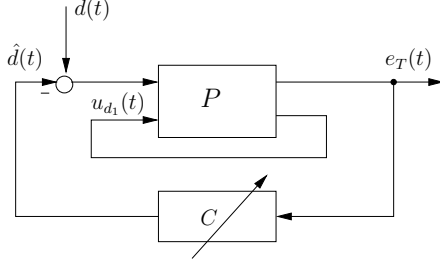


Fig. 2. The time-varying controller  $C$  cancels the time-varying disturbance to a time-varying system  $P$ .

Controller  $C$  synthesizes an estimate  $\hat{d}(t)$  of the disturbance from the error  $e_T(t)$  between the tension output and the desired tension to try to cancel the actual disturbance  $d(t)$ .  $C$  is depicted in the dashed box in Fig. 3 through which the signal  $\hat{d}(t)$  is generated. The algorithm is based on [2] with the difference that  $C_0$  is now time-varying:

$$C_0 = \left[ \begin{array}{cc} 0.5P_R(j\omega) & -0.5P_I(j\omega) \\ 0.5P_I(j\omega) & 0.5P_R(j\omega) \end{array} \right]^{-1} \Big|_{\omega=\omega_d(t)},$$

with  $P_R(j\omega)=\text{Re}(P(j\omega))$ ,  $P_I(j\omega)=\text{Im}(P(j\omega))$ , and  $\omega_d(t)$  is the frequency of the disturbance.  $C_1(s)$  and  $C_2(s)$  are two constant compensators chosen to guarantee the stability of the adaptation loops and the convergence speed of the adapted parameters [2].

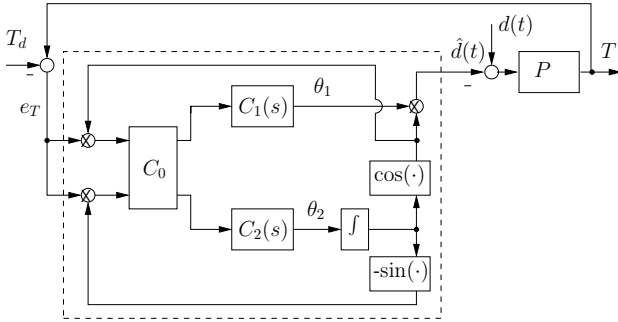


Fig. 3.  $C_0$  is a time-varying controller to adapt the magnitude  $\theta_1$  and the time-varying frequency  $\theta_2$  of the disturbance.

We implement a unit time-varying sinusoid signal as the reel eccentricity disturbance of the takeup reel and assume the frequency of the disturbance varies at a constant rate  $a$ . The tape tangential velocity is kept at 5 m/sec. Initially, the takeup reel is empty and the frequency of the disturbance is 56.8 Hz. The radius of the reel increases continuously until it reaches the maximum value and the frequency is 28.3 Hz. This whole process takes 30 seconds. Thus the initial frequency is 357 rad/sec and  $a = -5.9667 \text{ rad/sec}^2$ . The magnitude of the disturbance is assumed to be constant at 1.

The two constant controllers are selected as  $C_1(s) = \frac{20}{s}$  and  $C_2(s) = \frac{100(13s+100)}{s(s+60)}$  so that the poles of the two

adaptation loops are stable and at the same time, the convergence speed is acceptable. The selection of the poles is a tradeoff between the convergence speed and the oscillation dynamics during the adaptation period. We choose the initial values of the adapted magnitude and frequency to be 0.9 and 340 rad/sec, respectively. Simulation results of the time-varying controller algorithm are shown below in Fig. 4. The tension error decreases by nearly 2 orders of magnitude within 0.4 sec of when the disturbance with time-varying frequency is applied to the tape system. The magnitude also converges to nearly 1 within 0.4 sec and the frequency follows the linearly time-varying frequency of the disturbance afterwards.

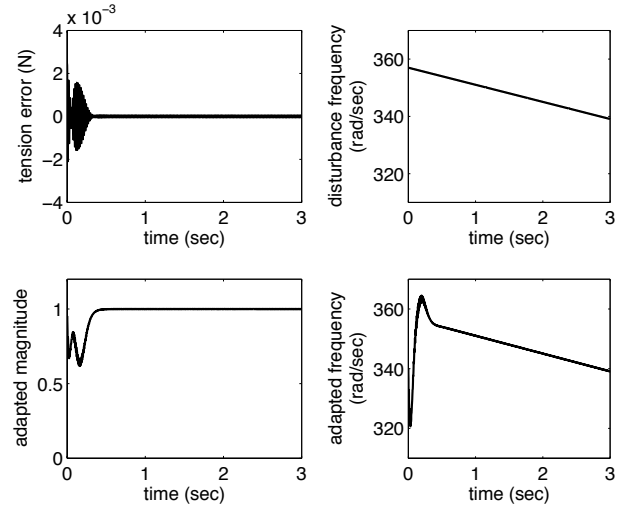


Fig. 4. The tension error under a disturbance with time-varying frequency is reduced by nearly 2 orders of magnitude within 0.4 seconds. The frequency of the disturbance from the reel eccentricity decreases at a constant rate. The adapted magnitude and frequency follows that of the disturbance, respectively.

### C. Gradient Descent on Squared Error

A discrete-time adaptive disturbance cancellation algorithm to cancel runout disturbances with fixed frequencies in hard disk drives is developed in [7]. We extend this algorithm to reject reel eccentricity disturbances in tape systems, which have time-varying frequencies. Unlike the algorithm discussed in section III-B, the parameter update rule here is a gradient descent based on squared error. Another difference is that in this algorithm, the reel eccentricity disturbance is considered as an output disturbance:

$$d_o(t) = A_{d_o} \cos(\omega_d(t)t), \quad \dot{\omega}_d(t) = a.$$

The control scheme is depicted in Fig. 5. The output  $y$  that contains the magnitude and frequency information of the disturbance  $d_o(t)$  activates the adaptive controllers  $G_1$  and  $G_2$  to synthesize the input signal  $u_o$ . Ideally, the plant's response to  $u_o$  would cancel the output disturbance  $d_o$  and hence  $y$  goes to zero. We call such an ideal input  $\bar{u}_o$ .

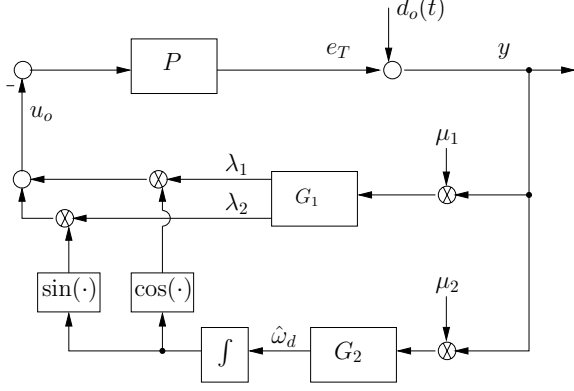


Fig. 5.  $G_1$  and  $G_2$  represent the parameter update rules and synthesize  $u_o$  from the output  $y$  to cancel the disturbance  $d_o$ .

Intuitively, to cancel the pure sinusoid output disturbance  $d_o(t)$ , the input  $u_o$  should be of the form  $A(t) \cos(\hat{\omega}_d(t)t + \phi(t))$ , where  $\hat{\omega}_d(t)$  is the adapted value of  $\omega_d(t)$ .  $A(t)$  and  $\phi(t)$  cancel the magnitude change and the phase loss of the input due to the tape system, respectively. Define

$$\begin{aligned} \lambda &= [\lambda_1, \lambda_2] = [A(t) \cos(\phi(t)), -A(t) \sin(\phi(t))], \\ \eta(\theta) &= [\cos \theta, \sin \theta]^T, \\ \hat{\varphi}(t) &= \hat{\omega}_d(t)t, \end{aligned}$$

then  $u_o = \lambda \eta(\hat{\varphi}(t))$ . The update rules [7] of the adapted parameter  $\lambda$  and  $\hat{\omega}_d$  are

$$\begin{aligned} \lambda(k) &= \lambda(k-1) - \mu_1 \left( \frac{\partial E^2}{\partial \lambda} \right), \\ \hat{\omega}_d(k) &= \hat{\omega}_d(k-1) - \mu_2 \left( \frac{\partial E^2}{\partial \hat{\omega}_d} \right), \end{aligned}$$

where  $E^2 = (u_o - \bar{u}_o)^2$ , the square of the difference between the synthesized input and the ideal input, and  $\mu_i$  is the adaptive step size gain. In our case, the time-varying nature of the disturbance frequencies introduces the variation of the magnitude and phase of the plant. However, the Bode plot of the plant  $P$  (Fig. 6) shows that the magnitude of the frequency response of the plant at the disturbance frequencies, ranging from  $\omega_1$  to  $\omega_2$ , can be considered as a constant at 0.0019 while the phase depends on the frequency. Thus, the adaptive update rules we use are

$$\begin{aligned} \lambda(k) &= \lambda(k-1) - \mu_1 \eta(\hat{\varphi}(k-1) + \hat{\varphi}(k-1)) y(k-1), \\ \hat{\omega}_d(k) &= \hat{\omega}_d(k-1) - \mu_2 \lambda(k-1) \dot{\eta}(\hat{\varphi}(k-1)) y(k-1). \end{aligned}$$

where

$$\hat{\varphi} = \angle P(j\omega)|_{\omega=\hat{\omega}_d}$$

and the synthesized input is

$$u_o(k) = \lambda(k) \eta(\hat{\varphi}(k)).$$

In the simulation evaluations, we choose the sampling time to be  $T_s = 0.0001$  sec and the output disturbance is  $d_o(t) = 0.0019 \cos(\omega_d(t)t)$  N with

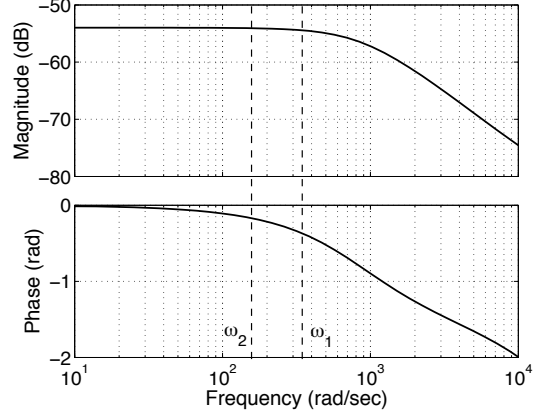


Fig. 6. The bode plot of  $P$  shows that within the range of  $\omega_d(t)$ , the magnitude is approximately constant while the phase changes.

$\omega_d(t) = 357 - 5.9667t$  rad/sec, where the frequency of the disturbance  $\omega_d(t)$  varies in the same way as discussed in section III-B and the output disturbance  $d_o(t)$  here is an equivalent to the unit input disturbance  $d(t)$  there. The initial value of the adapted frequency  $\hat{\omega}_d$  is chosen to be 340 rad/sec, as in the simulation in section III-B.  $\mu_1$  and  $\mu_2$  are empirically chosen to ensure the convergence speed and the stability [7]. The simulation results with  $\mu_1 = 1$  and  $\mu_2 = 50$  is illustrated in Fig. 7. The tension error decreases by nearly 2 orders of magnitude within 0.5 sec.

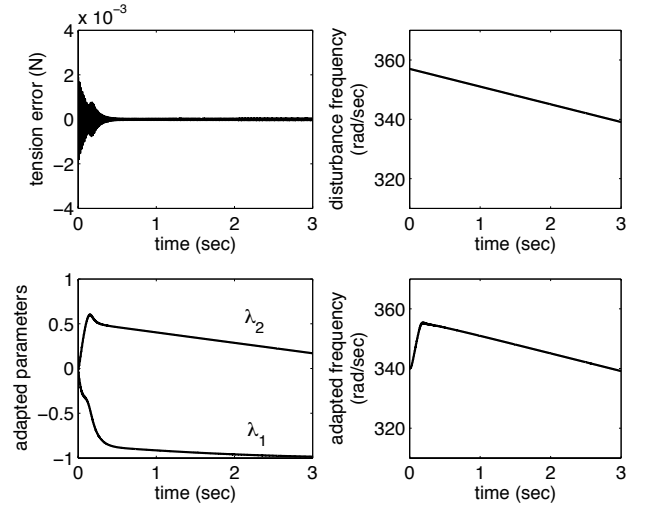


Fig. 7. The output disturbance is reduced by about 2 orders of magnitude within 0.5 seconds. The adapted frequency follows the linearly time-varying frequency of the disturbance after 0.2 seconds without any overshoot.

#### IV. DISCUSSION, CONCLUSIONS, AND FUTURE WORK

Two adaptive control algorithms that account for time-varying reel eccentricity disturbances in tape systems have been designed and evaluated. The time-varying controller

algorithm is designed in the continuous-time domain and it adapts the magnitude and the frequency of the input disturbance and synthesizes an inverse signal to reject the disturbance. The gradient descent algorithm in the discrete-time domain rejects the output disturbance by synthesizing an input signal to which the plant output response is the inverse of the disturbance. The simulation results show that both algorithms effectively reject the reel eccentricity disturbances with time-varying frequencies. Implemented on the same model of a tape system, with the same effective almost periodic disturbance, the disturbances in both algorithms are reduced by about 2 orders of magnitude within 0.5 seconds.

There are, however, several differences, advantages, and disadvantages of the two algorithms. The time-varying controller algorithm involves more dynamics during the convergence process as both the adapted magnitude and the adapted frequency oscillate. In the gradient descent algorithm, although the frequency adaptation loop converges about 2 times faster than that in the time-varying controller algorithm, the tension error in the gradient descent approach reaches steady-state later than with the time-varying controller algorithm since the adapted parameters  $\lambda_1$  and  $\lambda_2$  continue to vary to cancel the time-varying phase of the plant. The computational complexity of the gradient descent algorithm is higher than the time-varying controller approach because it calculates 3 adaptive parameters ( $\lambda_1$ ,  $\lambda_2$ , and  $\hat{\omega}_d$ ) in each iteration while the time-varying controller algorithm calculates 2 parameters ( $\theta_1$  and  $\theta_2$ ). Future work includes developing a discrete-time implementation of the time-varying controller approach and further comparing it with the discrete-time gradient descent algorithm.

We have thus far only implemented the control schemes to reject one disturbance, while in tape systems two (or more) different time-varying disturbances are induced by reel eccentricities due to the two reels. An extended scheme that cancels two (or more) distinct disturbances simultaneously will improve the performance of the tension control in real tape systems. In this paper, we have also assumed perfect feedback linearization, resulting in a time-invariant plant as used in the simulations. Future work will investigate the effects of model uncertainty as well as how to efficiently include multiple frequencies that are components of more complex reel eccentricity disturbances. Initial results investigating the robustness of the method of section III-B to model uncertainty are given in [9]. Future work will also combine control techniques to address air entrainment, parameter uncertainties, as well as reel eccentricities to achieve better overall performance in tape systems.

## REFERENCES

- [1] M. Baumgart and L. Pao, "Robust Lyapunov-based feedback control of nonlinear web-winding systems," *Proc. IEEE Conference on Decision and Control*, December 2003, pp. 6398-6405.
- [2] M. Bodson and S. Douglas, "Adaptive algorithms for rejection of periodic disturbances with unknown frequency," *Automatica*, vol. 33, no. 12, December 1997, pp. 2213-2221.
- [3] M. Bodson, J. Jensen, and S. Douglas, "Active noise control for periodic disturbances," *IEEE Trans. Control Systems Technology*, vol. 9, no.1, January 2001, pp. 200-205.
- [4] M. Bodson, A. Sacks, and P. Khosla, "Harmonic generation in adaptive feedforward cancellation schemes," *Proc. IEEE Conference on Decision and Control*, December 1992, pp. 1261-1266.
- [5] L. Brown and Q. Zhang, "Periodic disturbance cancellation with uncertain frequency," *Automatica*, vol. 40, no. 4, April 2004, pp. 631-637.
- [6] B. Francis and B. Wonham, "The internal model principle of control systems," *Automatica*, vol. 12, no. 5, 1976, pp. 457-465.
- [7] U. Hand, "A new adaptive algorithm for disturbance cancellation in hard drives," M.S. Thesis, University of Colorado at Boulder, Boulder, CO, 2000.
- [8] S. Hara, Y. Yamamoto, T. Omata, and M. Nakano, "Repetitive control system: a new type servo system for periodic exogenous signals," *IEEE Trans. Automatic Control*, vol. 33, no.7, July 1988, pp. 659-668.
- [9] V. Kulkarni, L. Pao, and H. Zhong, "Robust rejection of periodic and almost periodic disturbances," *Proc. 16th IFAC World Congress*, July 2005.
- [10] Y. Lu and W. Messner, "Robust servo design for tape transport," *Proc. IEEE International Conference on Control Applications*, September 2001, pp 1014-1019.
- [11] P. Mathur and W. Messner, "Controller development for a prototype high-speed low-tension tape transport," *IEEE Trans. Control Systems Technology*, vol. 6, no. 4, July 1998, pp. 534-542.
- [12] A. Sacks, M. Bodson, and W. Messner, "Advanced methods for repeatable runout compensation," *IEEE Trans. Magnetics*, vol. 31, no. 2, March 1995, pp. 1031-1036.
- [13] Y. Xu, M. Mathelin, and D. Knittel, "Adaptive rejection of quasi-periodic tension disturbances in the unwinding of a non-circular roll," *Proc. American Control Conference*, vol. 5, May 2002, pp. 4009-4014.